Body mass dependence of oxidative phosphorylation efficiency in liver mitochondria from mammals

Mélanie Boël, Yann Voituron, Damien Roussel

Body mass dependence of oxidative phosphorylation efficiency in liver mitochondria from mammals

Boël Mélanie [1, 2 *], Voituron Yann [1 #], and Roussel Damien [1 * #]

[1] LENHA, UMR 5023 CNRS, Université de Lyon; ENTPE, Lyon, France

[2] UMR 6553, Univ Rennes, CNRS, ECOBIO (Ecosystèmes, Biodiversité, Évolution), Rennes, France

[#] These authors equally contributed to this work

*To whom correspondence should be addressed: LEHNA, UMR 5023 CNRS, Université Claude Bernard Lyon 1, Bâtiment Charles Darwin C, 69622 Villeurbanne cedex, France.

Tel: +33 4 72 43 16 51; E-mail: melanie.boel@live.com, damien.roussel@univ-lyon1.fr

Abstract

In eukaryotes, the performances of an organism are dependent on body mass and chemically supported by the mitochondrial production of ATP. Although the relationship between body mass and mitochondrial oxygen consumption is well described, the allometry of the transduction efficiency from oxygen to ATP production (ATP/O) is still poorly understood. Using a comparative approach, we investigated the oxygen consumption and ATP production of liver mitochondria from twelve species of mammals ranging from 5g to 600 kg. We found that both oxygen consumption and ATP production are mass dependent but not the ATP/O at the maximal phosphorylating state. The results also showed that for sub-maximal phosphorylating states the ATP/O value positively correlated with body mass, irrespective of the metabolic intensity. This result contrasts with previous data obtained in mammalian muscles, suggesting a tissue-dependence of the body mass effect on mitochondrial efficiency.

Introduction

Irrespective of the organization level, i.e., from cells to ecosystems, the body mass of organisms influences a multitude of biological processes. The metabolic rate of individuals is one such biological process, which co-varies with the body mass as $MR = a \times BM^b$; where MR is the metabolic rate, BM the body mass, "a" the intercept at the origin and "b" the scaling exponent (Schmidt-Nielsen, 1984). The value of the scaling exponent "b" depends on phylogeny and several other parameters (e.g., food intake, habitat, etc.) but remains less than 1 (White et al., 2007; Glazier, 2008; Makarieva et al., 2008), indicating that larger organisms consume less oxygen per unit of body mass to ensure their homeostasis than do smaller organisms. Among the various hypotheses seeking to explain the mechanistic basis of this power law for interspecies metabolic scaling, the allometric cascade suggests that it results from the sum of various cellular and mitochondrial properties involved in ATP turnover (Hulbert and Else, 2000; Darveau et al., 2002; Hochachka et al., 2003; Weibel et al., 2004).

In tissues from aerobic organisms, mitochondrial metabolism provides most of the cellular energy needs in the form of ATP *via* oxidative phosphorylation (Rolfe and Brown, 1997). During oxidative phosphorylation, mitochondria consume oxygen to establish an electrochemical gradient of protons that is secondarily consumed by ATP synthase to phosphorylate ADP into ATP. Mitochondrial oxygen consumption, which is linearly linked to ATP synthesis (Beavis and Lehninger, 1986; Fontaine et al., 1996), decreases with body mass in endotherms (Porter and Brand, 1995; Brand et al., 2003; Mélanie et al., 2019). However, part of the mitochondrial respiration is not coupled to ATP synthesis, since the electrochemical gradient of protons can also be consumed by proton leak pathways (Rolfe and Brown, 1997). Such futile proton cycling across the inner mitochondrial membrane, leading to local heat production, contributes to a large proportion of the cellular metabolic rate, from 20% in hepatocytes to 52% in resting skeletal muscle (Porter and Brand, 1995; Rolfe and

Brand, 1996), thus amounting to a significant contributor to the basal metabolic rate in whole animals (Porter, 2001). It has been reported that both maximal proton leak activity and the inner membrane proton conductance of mitochondria are negatively related to body size and positively related to the basal metabolic rate in endotherms (Porter and Brand, 1993; Brand et al., 2003; Polymeropoulos et al., 2012, Mélanie et al., 2019). Since proton leak triggers mitochondrial inefficiency, it is expected that large animals should have a higher mitochondrial efficiency than smaller species.

The mitochondrial coupling efficiency (ATP/O ratio), i.e., the amount of ATP produced per molecule of oxygen consumed, is of physiological and ecological importance as it can drive/constrain organism performances in a constantly changing environment (Brand, 2005; Salin et al., 2015; Bourguignon et al., 2017). Despite the negative relationships between mitochondrial proton leak conductance and body size, the relative contribution of proton leak activity to the resting respiration of hepatocytes remains independent of body mass in both mammals and birds (Porter and Brand, 1995; Else et al., 2004). This results in the effective coupling efficiency for hepatocytes being independent of body mass. Similarly, the maximal coupling efficiency of skeletal muscle mitochondria from large and small mammals is independent of body mass (Mélanie et al., 2019; Boël et al., 2020). Nevertheless, the allometric relationship between mitochondrial coupling efficiency and body mass also depends on the level of oxidative phosphorylation activity, becoming all the more positive when mitochondrial activity decreases toward a non-phosphorylating state (Mélanie et al., 2019). *In situ*, the contribution of mitochondrial proton leak to respiration of perfused skeletal muscle has been shown to increase from 34% in the working state to 52% in the resting state (Rolfe and Brand, 1996; Rolfe et al., 1999). Thus, the dependence of the coupling efficiency of muscle mitochondria with the level of oxidative phosphorylation activity may reflect the fact that aerobic metabolism of skeletal muscle can increase 10-fold between a loosely

coupled resting state (high proton leak activity and low mitochondrial efficiency) and a tightly coupled active state (low proton leak activity and high mitochondrial efficiency). In contrast, the contribution of mitochondrial proton leak to hepatocyte respiration only changes slightly, from 22% in the working state up to 26% in the resting state (Rolfe and Brand, 1996; Rolfe et al., 1999). This may reflect the fact that liver is a highly active organ *in vivo*, as is hence constantly in a tightly-coupled active state.

The question raised by these results is whether the mitochondrial coupling efficiency of liver is also dependent on the metabolic intensity. We predict that body mass would mainly influence the mitochondrial coupling efficiency of liver at low oxidative phosphorylation activity, but to a lower extend than that reported in skeletal muscle mitochondria. Hence, the aim of the present study was to investigate 1) the allometric relationship between body mass and the coupling efficiency of liver mitochondria from mammals, using mammals with a wide mass range, from pygmy and harvest mice weighing 7 g to 500 kg bovine, and 2) its dependence on the level of oxidative phosphorylation activity.

Materials and Methods

All experiments were conducted in accordance with animal care guidelines of the Ministère de la Recherche et de l'Enseignement Supérieur.

Biological samples

For this experiment, thirteen mammalian species were selected, from 6 g (African pygmy mouse and Harvest rat) to 550 kg (bovine), and all individual were males. Liver tissue was freshly acquired and used for mitochondrial extraction. African pygmy mice (*Mus minutoides, n*=6), feral mice (*Mus musculus, n*=10) were obtained from laboratories (ISEM, Montpellier France for African pygmy mice*;* LBBE, Lyon, France for feral mice) while

Harvest rat (*Micromys minutus, n*=8) were obtained from Jardin Zoologique de la Citadelle (Besançon, France), and they are killed by cervical dislocation. Striped mice (*Rhabdomys pumilio, n*=5), European hamster (*Cricetus cricetus, n*=8), Golden hamsters (*Mesocricetus auratus, n*=8) and black rats (*Rattus rattus, n*=8) were killed under isoflurane-induced general anesthesia and were obtained from laboratories (IPHC, Strasbourg, France for striped mice and European hamster; Chronobiotron, Strasbourg, France for Golden hamster; Jardin Zoologique de la Citadelle, Besançon, France for black rat). Concerning liver tissues for bovine (*Bos taurus, n*=8), horses (*Equus caballus, n*=4) and sheep (*Ovis aries, n*=6), they were freshly obtained from a local slaughter house (Cibevial, Corbas, France). Fresh tissue for all other mammals was obtained from pest control (Nutria, *Myocastor coypus, n*=3), local farmers (rabbits, *Oryctolagus cuniculus, n*=6) or Fondation Pierre Vérot at Saint-André-de-Corcy, France (boar, *Sus scrofa, n*=5).

Mitochondrial isolation

Liver tissue was freshly dissected and placed in an ice-cold isolation buffer (250 mM sucrose, 1 mM EGTA, 20 mM Tris-base, 1% de BSA, pH 7.3). Liver tissue was rapidly ground with a Potter-Elvehjem homogenizer and then centrifuged at 1,000 × g for 10 min. The pellet was discarded and the supernatant was centrifuged at 1,000 × g for 10 min in isolation buffer without BSA. The resulting supernatant was filtered through cheesecloth and then centrifuged at 8,700 × g for 10 min to pellet the mitochondria. The pellet was resuspended in isolation buffer and centrifuged at 8,700 × g for 10 min. This last step was performed twice. All steps were carried out at 4°C (Salin et al., 2010). The mitochondrial suspension was then used fresh to measure bioenergetics parameters, and an aliquot was frozen and stored at -80°C until the protein concentration was determined by standard BCA

kit assay. For the African pygmy mouse, liver samples from three or four individuals were pooled for each mitochondrial preparation.

Mitochondrial bioenergetics parameters

Mitochondrial oxygen consumption and ATP synthesis were assayed at 37°C in 500 µL of respiratory buffer (120 mM KCl, 5 mM KH_2PO_4, 1 mM EGTA, 2 mM $MgCl_2$, 20 mM glucose, 1.6 U/mL hexokinase, 0.3 % essentially free-fatty acid bovine serum albumin (w/v) and 3 mM Hepes, pH 7.4). The mitochondrial oxygen consumption was measured in a glass cell fitted with a Clark oxygen electrode (Rank Brothers Ltd, UK) in the presence of a mixture of respiratory substrates (5 mM pyruvate/2.5 mM malate/5 mM succinate). Thereafter, different steady states of phosphorylation were obtained by adding different concentrations of ADP (10, 25, 100 and 500 µM). The phosphorylating respiration rates were recorded for 3 min, then four 100 µL aliquots of mitochondrial suspension were withdrawn every 30 seconds and immediately quenched in 100 µL of ice-cold perchloric acid solution (10% $HClO_4$, 25 mM EDTA). The denatured proteins were then centrifuged at 20,000 × g for 5 min (4°C), and 180 µL of the resulting supernatants were neutralized with KOH solution (2 M KOH, 0.3 M MOPS). The neutralized samples were centrifuged at 20,000 × g for 5 min (4°C), and the mitochondrial ATP production was determined from the glucose-6-phosphate content of the resulting supernatants (Teulier et al., 2010). The glucose-6-phosphate content was determined by spectrophotometry at 340 nm in assay medium (7.5 mM $MgCl_2$, 3.75 mM EDTA, 50 mM triethanolamine–HCl, pH 7.4) supplemented with 0.5 mM NAD^+ and 0.5 U glucose-6-phosphate dehydrogenase from *Leuconostoc mesenteroides,* at room temperature (Lang and Michal, 1974). To verify that the ATP synthesis rate is specifically linked to the mitochondrial ATP synthase activity, the oxygen consumption and ATP synthesis rates were also measured in the presence of oligomycin (2 $\mu g.mL^{-1}$). The respiratory control ratio (RCR)

was calculated by dividing the oxygen consumption rate measured at the maximal phosphorylating state over that measured at the oligomycin-induced non-phosphorylating state.

Enzyme activities and mitochondrial content

The cytochrome-c oxidase activity was the maximal respiration rate measured in freshly isolated liver mitochondria respiring on ascorbate (4 mM) and N,N,N',N'-tetramethyl-p-phenylene-diamine (50 µM) in respiratory buffer (120 mM KCl, 5 mM KH_2PO_4, 1 mM EGTA, 2 mM $MgCl_2$, 0.3% essentially free-fatty acid bovine serum albumin (w/v) and 3 mM Hepes, pH 7.4) supplemented with 10 µM antimycin, 2 $\mu g.mL^{-1}$ oligomycin, and 2 µM carbonyl cyanide p-trifluoromethoxyphenylhydrazone (FCCP). The cytochrome-c oxidase activity was determined in liver mitochondria of eleven mammalian species: harvest rat (*n*=8), African pygmy mouse (*n*=6), feral mouse (*n*=5), striped mouse (*n*=5), golden hamster (*n*=8), black rat (*n*=8), European hamster (*n*=8), rabbit (*n*=6), nutria (*n*=3), sheep (*n*=6), and bovine (*n*=4).

Citrate synthase activity from frozen mitochondria or liver tissue was measured spectrophotometrically at 37°C. Frozen mitochondria were thawed and diluted 1:4 in 100 mM phosphate buffer containing 2 mM EDTA. The frozen liver tissues were ground in 300 mM phosphate buffer containing 10% bovine serum albumin. The crushed liver was prepared by three freeze/thaw cycles before being diluted 1:2 in 100 mM phosphate buffer containing 2 mM EDTA. The citrate synthase activity was then measured at 412 nm in reaction medium (100 mM TRIS buffer, 100 µM 5,5'-dithiobis(2-nitrobezoic acid), 300 µM acetyl-CoA; pH 8) supplemented with 40-120 $\mu g.mL^{-1}$ of liver sample or with 20-60 µg $protein.mL^{-1}$ of mitochondrial sample. After 3 min of incubation, the reaction was started by the addition of 500 µM oxaloacetate, and the reduction was followed at 412 nm (Medja et al., 2009). The

enzymatic activity was quantified using an extinction coefficient set at 13.6 $mmol.l^{-1}.cm^{-1}$. The mitochondrial content was expressed in mg of mitochondrial protein per g of liver and was estimated by the ratio of the citrate synthase activities measured in liver tissue (CS_{liver}) over the corresponding activity measured in isolated mitochondria (CS_{mito}). The mitochondrial citrate synthase activity was determined in nine mammalian species: harvest rat (*n*=4), African pygmy mouse (*n*=6), feral mouse (*n*=7), striped mouse (*n*=5), black rat (*n*=9), European hamster (*n*=8), rabbit (*n*=5), nutria (*n*=3), equine (*n*=4), and bovine (*n*=5). The activity of citrate synthase in liver was not determined in the three smallest species (harvest rat, pygmy mouse, and feral mouse) because all of the liver sampling was used to isolate mitochondria. Therefore, liver citrate synthase activity, and thus the mitochondrial content, was measured in seven mammalian species only.

Statistical analyses

R software 4.1.0 (R Foundation for Statistical Computing, Vienna, Austria, 2018) was used for all statistical analyses. The combined effect of mitochondrial ATP synthesis and body mass on mitochondrial efficiency (ATP/O ratio) was analyzed by a linear model (LM), with body mass and the mitochondrial ATP synthesis as fixed factors, after verifying that there was no interaction between the two factors. After a log 10 transformation of the data, allometric relationships between body mass and mitochondrial bioenergetics parameters, i.e., oxygen consumption and ATP production rates, as well as the efficiency and enzyme activities (CS_{liver}, CS_{mito}, and COX) were analyzed by a linear model (LM), with body mass as a fixed term. Normality and homoscedasticity criteria for the model's residues were then checked by a Shapiro-Wilk normality test coupled to the plotting diagnostics for an LM object. Allometric relationships were also analyzed after correction of the data by the Phylogenetic Independent Contrast model in order to obtain the phylogenetically independent data, by using the "ape" package that follows the phylogenetical correction method proposed

by Felsenstein (Mélanie et al., 2019). The mammal phylogenetic tree used for these analyses was created from the mammal phylogenetic super tree proposed by (Fritz et al., 2009) using the "phytools" package (Figure 1). Both types of statistical analyses, with data corrected or not corrected by phylogeny, are presented in the article, with p-values < 0.05 considered statistically significant. The results are presented as means ± s.d.

Results

Mitochondrial oxygen consumption and ATP synthesis rates

Figure 2 shows the linear relationship between the rates of ATP synthesis and oxygen consumption in liver mitochondria from each of the thirteen mammalian species. The rates of oxygen consumption at maximal phosphorylating (the highest point to the right of the linear relationships in Fig. 2) and non-phosphorylating states (measured in the presence of oligomycin and corresponding to the intercepts with the *x*-axis in Fig. 2) were negatively related to mammalian body mass (J_O; $F_{(1,11)} = 26.745$, $p < 0.001$; J_{oligo}; $F_{(1,11)} = 27.335$, $p < 0.001$; Fig. 3A). The respiratory control ratios (RCR) ranged from 2.3 to 4.6, with a mean of 3.2, and did not depend on body mass ($F_{(1,11)} = 1.468$, $p = 0.25$) (Fig. 3A). The RCR is often used as a functional index of mitochondrial preparations, with low RCR values (<1) usually indicating dysfunction (Brand et al., 2003; Brand and Nicholls, 2011). The RCR values of the present study fall within the range of values previously published for liver mitochondria respiring on succinate in birds (from 2.4 to 5, mean value of 3.8; Brand et al., 2003), and are in the lower range of values reported in mammals (2.9 to 7.8; Barger et al., 2003; Boël et al., 2020; Brown and Staples, 2010; Dufour et al., 1996; Mollica et al., 2005; Polymeropoulos et al., 2012; Roussel et al., 2004). Thus, this result indicates that liver mitochondria from larger species were not better or worse than those from smaller species. The maximal rate of ATP synthesis also decreased with increasing body mass (J_{ATP}; $F_{(1,11)} = 22.439$, $p < 0.001$; Fig. 3B).

However, these relationships between mitochondrial fluxes and mammal body masses failed to reach significance when phylogeny was considered (J_{oligo}: $F_{(1,11)} = 2.988$, $p = 0.11$; J_O: $F_{(1,11)} = 3.986$, $p = 0.071$; J_{ATP}: $F_{(1,11)} = 4.037$, $p = 0.070$).

Mitochondrial coupling efficiency (ATP/O)

Since the oxygen consumption and ATP synthesis fluxes exhibited similar scaling exponents when calculated at the maximum phosphorylating activity, the ratio between the maximal rates of ATP synthesis (J_{ATP}) and the corresponding phosphorylating oxygen consumption (J_O), i.e. the effective mitochondrial coupling efficiency, was independent of body mass ($ATP/O_{max} = 1.22 \times mass^{-0.012}$; $F_{1,11} = 1.703$, $p = 0.22$ and $F_{1,11} = 0.761$, $p = 0.40$ when phylogeny was considered). The slopes of the linear relationships shown in Fig. 2 are a measure of the maximum P/O ratio of mitochondrial oxidative phosphorylation, and their values were also independent of body mass (Fig. 3B). Nevertheless, the effective mitochondrial coupling efficiency increased non-linearly with the rate of ATP synthesis and also differed between the mammalian species (Fig. 4A). The data in Figs. 2 and 4A clearly show that to produce the same amount of ATP, mitochondria from smaller mammals consume more oxygen and thus have lower coupling efficiency than mitochondria from larger species. This is well illustrated in Fig. 4B, which shows the effective coupling efficiencies calculated at specific ATP synthesis rates. Hence, the mitochondrial coupling efficiency co-varies positively with body mass in mammals ($F_{(1,11)} = 22.652$; $p < 0.001$ for ATP/O_{50}, $F_{(1,11)} = 24.330$; $p < 0.001$ for ATP/O_{25} and $F_{(1,11)} = 25.561$; $p < 0.001$ for ATP/O_{10}), without interaction between the metabolic intensity effect and body mass ($F_{(2)} = 0.637$; $p = 0.54$) (Fig. 4B). Of note, significance of the whole relationship was not reached when the data were made phylogenetically independent ($F_{(1,11)} = 1.638$; $p = 0.23$ for ATP/O_{50}, $F_{(1,11)} = 2.118$; $p = 0.17$ for ATP/O_{25} and $F_{(1,11)} = 2.510$; $p = 0.14$ for ATP/O_{10})

Mitochondrial enzyme activities

Fig. 5 shows that the activities of cytochrome-c oxidase (COX_{mito}; Fig. 5A) and citrate synthase (CS_{mito}; Fig. 5B) in isolated mitochondria decreased significantly with increasing body mass ($F_{(1,9)} = 19.99$; $p = 0.002$ for COX_{mito} and $F_{(1,8)} = 26.611$; $p < 0.001$ for CS_{mito}), even when the phylogenetic link between species was considered ($F_{(1,9)} = 7,112$; $p = 0.026$ for COX_{mito}, $F_{(1,8)} = 19.146$; $p = 0.002$ for CS_{mito}). Similarly, the citrate synthase activity of liver (CS_{liver}) also negatively correlated with body mass in mammals ($F_{(1,5)} = 9.075$, $p = 0.024$; Fig. 5B), but the negative relationship failed to reach significance when phylogeny was taken into account ($F_{(1,5)} = 4.881$; $p = 0.069$). The mitochondrial content of liver tended to decrease with increasing body mass ($F_{(1,5)} = 5.4155$, $p = 0.068$ without considering phylogeny, and $F_{(1,5)} = 4.745$, $p = 0.081$ with phylogeny ; Fig. 5C).

Discussion

The present comparative study shows that body mass dependence of mitochondrial coupling efficiency depends on the level of oxidative phosphorylation activity of mitochondria in liver. It follows that liver mitochondria from smaller mammals exhibit lower coupling efficiencies than larger species when working at low intensity. Yet, the fundamental result of the current study is that the coupling efficiency of liver mitochondria are less flexible, maintaining higher ATP/O values than skeletal muscle mitochondria at low oxidative phosphorylation intensity.

The aerobic metabolism of individuals co-varies with body mass from the whole organism up to the cellular and sub-cellular levels (Hulbert and Else, 2000; Darveau et al., 2002; Hochachka et al., 2003; Weibel et al., 2004). The rate of oxygen consumption in cells and mitochondria, as well as the activities of oxidative enzymes (such as cytochrome-c oxidase, citrate synthase, succinate dehydrogenase, and malate dehydrogenase) from different tissues

negatively scales with body mass in endotherms (Krebs, 1950; Kunkel and Campbell, 1985; Fried and Tipton, 1953; Smith, 1956; Emmet and Hochachka, 1981; Porter and Brand, 1995; Brand et al., 2003; Mélanie et al., 2019). In addition, the high oxygen consumption of hepatocytes from small species is also partly due to a higher content/volume of mitochondria (Smith, 1956; Else and Hulbert, 1985; Porter and Brand, 1995). Here, we also report a negative scaling of mitochondrial content, mitochondrial fluxes (oxygen consumption and ATP production), and enzyme activities involved in oxidative metabolism (cytochrome-c oxidase and citrate synthase) with body mass in the liver of mammals.

Mitochondrial oligomycin-induced non-phosphorylating activity decrease with increasing body mass in mammals. In the presence of oligomycin, resulting in no ATP synthesis, the rate of proton leak-dependent oxygen consumption is maximal and mainly controlled by the proton conductance of the inner membrane (Rolfe et al., 1994; Dufour et al., 1996; Brand and Nicholls, 2011). This is in accordance with the negative allometric relationships between mitochondrial inner membrane proton conductance and animal body size reported in many taxa, including mammalian, marsupial, bird, and frog species (Porter and Brand, 1993; Brand et al., 2003; Polymeropoulos et al., 2012; Roussel et al., 2015). Since proton leak diverts energy away from ATP production, mitochondria of larger species should have a higher efficiency than those of smaller species. However, the relative proportion of mitochondrial oxygen consumption due to proton leak (19%) and phosphorylating system (68%) in resting hepatocytes has been reported to be constant whether mammalian species are large or small (Porter and Brand, 1995). This suggests that the mitochondrial effective coupling ratio for hepatocytes is overall independent of body mass (Porter and Brand, 1995). In the present study, the mitochondrial oxidative phosphorylation efficiency was determined straightforwardly by measuring ATP synthesis concurrently with the oxygen consumption at different steady states of metabolic activity in liver mitochondria (Fig. 2). In accordance with

data previously reported for skeletal muscle mitochondria (Mélanie et al., 2019), the rates of maximal ATP synthesis and associated oxygen consumption decreased as the body mass increased according to similar scaling exponents. Consequently, the ATP/O ratio calculated from these two fluxes at maximum phosphorylating state was independent of body mass. Although the oxygen consumed during the phosphorylating state is mainly used to drive ATP synthesis, proton leakage still occurs, contributing to 5%-20% of the phosphorylating oxygen consumption, depending on the respiratory substrate and the tissue (Brand et al., 1993; Rolfe and Brand, 1994; Lombardi et al., 2000; Barger et al., 2003; Roussel et al., 2004; Brown and Staples, 2010). The relatively constant values of ATP/O with body mass in skeletal muscle (Mélanie *et al.*, 2019) and liver (present study) indicate that the proportion of proton leak to phosphorylating respiration is the same for all of the investigated mammals. Hence, the effective amount of ATP synthesized per unit of oxygen consumed is optimal and independent of body mass in skeletal muscle and liver when their mitochondria synthesize ATP at a high rate.

However, our previous study on skeletal muscle mitochondria reported a more complex picture, whereby the mitochondrial coupling efficiency is independent of body mass at the maximum phosphorylating state and becomes positively dependent on body mass at submaximal oxidative phosphorylation activity (Mélanie *et al.*, 2019). In keeping with this, the mitochondrial coupling efficiency in liver becomes positively dependent on body mass at submaximal oxidative phosphorylation activity. For instance, when mitochondria are working very slowly, close to the basal state (i.e., synthesizing 10 nmol $ATP.min^{-1}.mg^{-1}$), the two smallest species (*Mus minutoides* and *Micromys minutus*) have less efficient mitochondria (ATP/O = 0.15 ± 0.04) than those of the two largest species (*Bos taurus* and *Equus caballus*; ATP/O = 0.39 ± 0.14; Fig. 4B). This implies that liver mitochondria from small mammal species may reduce their effective ATP/O ratio to lower values and thus exhibit a more

flexible coupling efficiency than larger species. The greater decline in the ATP/O ratio of liver mitochondria from smaller mammals could be explained by higher proton conductance of their inner membrane compared with that of larger mammals (Porter and Brand, 1993; Porter et al., 1996; Polymeropoulos et al., 2012). Interestingly, at low levels of oxidative phosphorylation activity, mitochondria from skeletal muscle are, on average, 35% less coupled than those from liver (Mélanie *et al.*, 2019; present study; see dashed line in Fig. 4B). In other words, mitochondria from skeletal muscle are "intrinsically" more thermogenic at low oxidative phosphorylation activity than mitochondria from liver. These data also suggest that skeletal muscle mitochondria display a more flexible coupling efficiency than liver mitochondria, further decreasing their ATP/O ratios at low activity. Again, such difference in ATP/O flexibility could be adequately explained by a difference in the mitochondrial inner membrane proton conductance, which is higher in skeletal muscle than in liver (Rolfe and Brand, 1994; Roussel et al., 2002; Barger et al., 2003; Mollica et al., 2005; Salin et al., 2010). This hypothesis is reinforced by *in situ* experiments, which show a higher contribution of mitochondrial proton leak to respiration in perfused skeletal muscle compared to that in hepatocytes at resting state, i.e. 52% in skeletal muscle *versus* 20%-26% in liver (Porter and Brand, 1995; Rolfe and Brand, 1996; Rolfe and Brand, 1999).

Conclusion

Body mass influences the level of mitochondrial coupling flexibility in both skeletal muscle and liver (Mélanie et al., 2019; present study). Hence, mitochondria from smaller mammals exhibit lower coupling efficiencies when working at low intensity compared to larger species. The present study also highlights tissue differences, with mitochondria from liver being less flexible, exhibiting a smaller range of ATP/O values than those of skeletal muscle. This difference in the flexibility may result from a difference in the metabolic scope between the

two tissues. Liver is a constantly active organ *in vivo*, contributing to vital homeostatic functions of the organism, whereas the activity of skeletal muscle can vary greatly according to the needs of organisms for locomotion or thermoregulation. On the one hand, skeletal muscle mitochondria can attain a high ATP/O ratio, allowing them to produce a large amount of energy in the form of ATP necessary to cope with the high energy demand of an intense physical effort such as escaping a predator. On the other hand, skeletal muscle mitochondria can reach lower ATP/O values at low mitochondrial activity compared to liver, which could be an interesting mechanism to generate heat at minimum cost for thermoregulation.

Figure legends

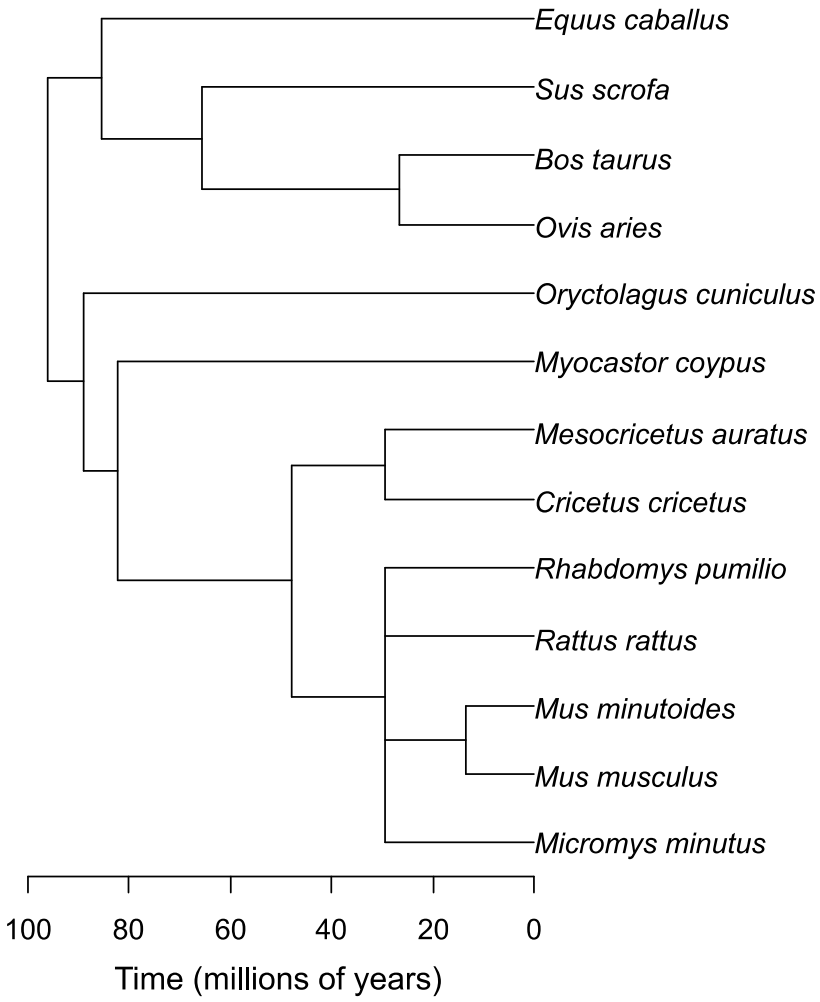

Figure 1: Phylogenetic tree for the thirteen mammalian species of the present study.

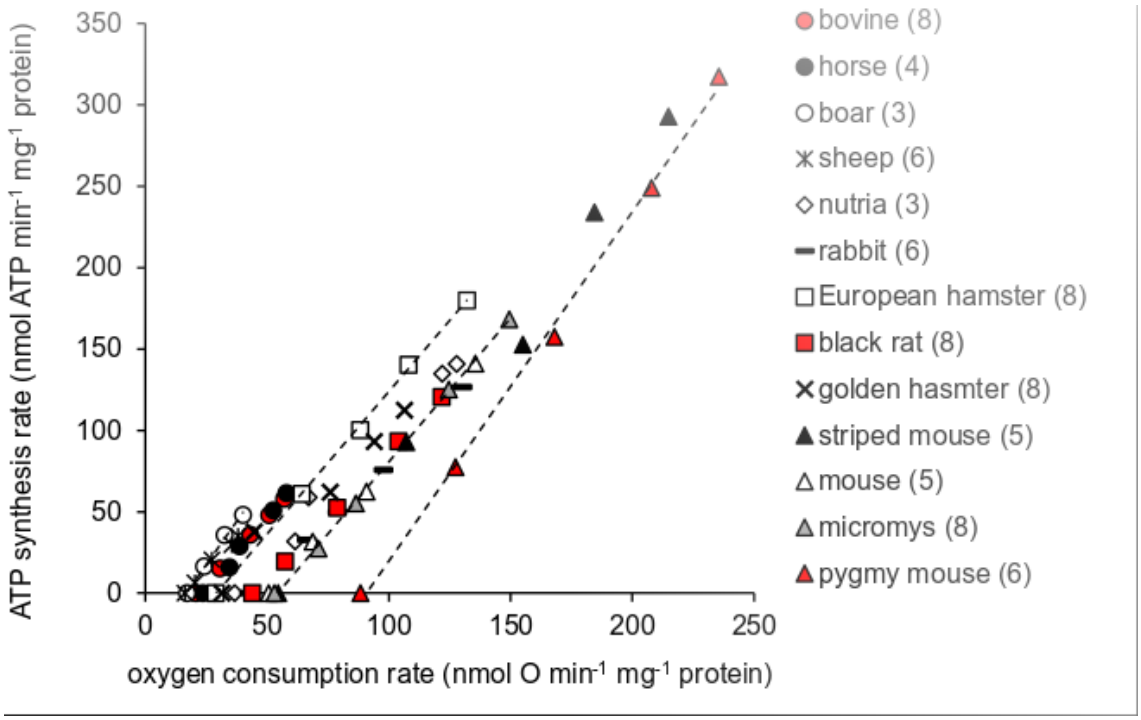

Figure 2: Mitochondrial oxidative phosphorylation activity. Relationship between the rates of ATP synthesis and corresponding oxygen consumption in liver mitochondria isolated from mammals of different body mass. Red symbols and dashed lines illustrate the linearity of the relationships for mammalian species taken to cover a wide range of body mass (from the left to the right on the graph: bovine, European hamster, black rat, and African pygmy mouse). Values are means from (n) independent mitochondrial preparations, with (n) indicated alongside the name of the species. Error bars (s.d.) have been omitted for clarity but were, on average, 29% for both the maximal oxygen consumption rate (ranging from 13% in *Micromys* to 49% in nutria) and the ATP synthesis rate (ranging from 20% in *Micromys* to 44% in black rat).

Figure 3: Body mass dependence of mitochondrial oxidative phosphorylation activity. A) Relationships between body mass and maximal phosphorylating oxygen consumption rate (J_O = 245 x mass$^{-0.12}$, r^2 = 0.71, black circles), oligomycin-induced basal non-phosphorylating oxygen consumption rate (J_{Ooligo} = 76 x mass$^{-0.11}$, r^2 = 0.71, white circles) and respiratory control ratio (RCR = 3.40 x mass$^{-0.017}$, r^2 = 0.12, grey circles). B) Relationship between body

mass and maximal ATP synthesis rate (J_{ATP} = 298 x mass$^{-0.14}$, r^2 = 0.68, black triangles) and the slope of the linear relationships shown in Fig. 2 (P/O = 1.70 x mass$^{0.0028}$, r^2 = 0.008, grey triangles). Values are means ± s.d. from (n) independent mitochondrial preparations (n is provided in Fig. 2 alongside the name of the species).

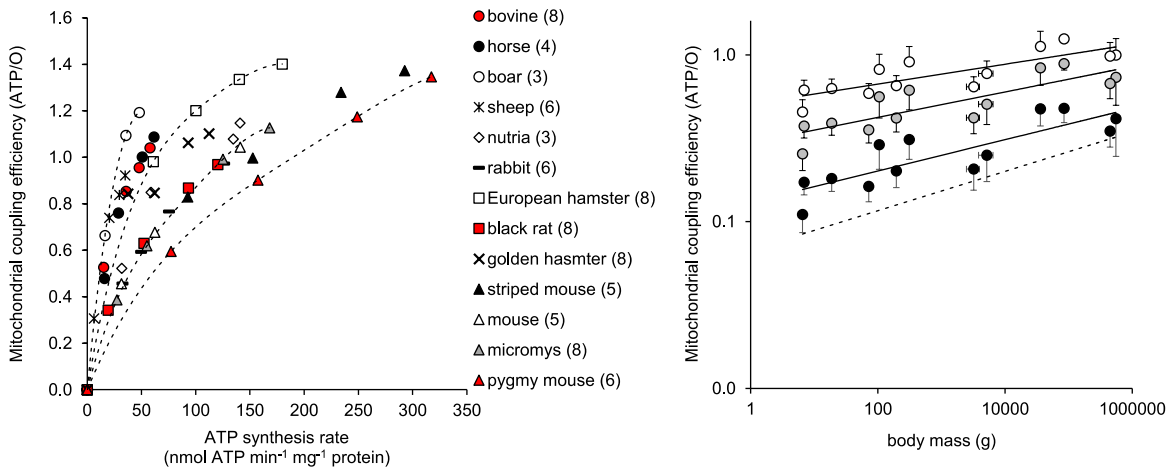

Figure 4: Body mass dependence of mitochondrial oxidative phosphorylation efficiency. A) Relationships between the effective coupling efficiency (ATP/O) and corresponding ATP synthesis in liver mitochondria isolated from mammals of different body mass. Red symbols and dashed lines illustrate the non-linearity of the relationships for mammalian species taken to cover a wide range of body mass (from left to the right on the graph: bovine, European hamster, black rat and African pygmy mouse). Values are means from (n) independent mitochondrial preparations, with (n) indicated alongside the name of the species. Error bars (s.d.) have been omitted for clarity but were, on average, 17% for the maximal ATP/O ratio (ranging from 2% in boar to 31% in equine). B) Relationships between body mass and effective coupling efficiency (ATP/O ratio) calculated for a given ATP synthesis rate at 50 nmol ATP.min^{-1}.mg^{-1} (ATP/O = 0.53 x mass$^{0.04}$, r^2 = 0.57, white circles); 25 nmol ATP.min^{-1}.mg^{-1} (ATP/O = 0.30 x mass$^{0.08}$, r^2 = 0.69, grey circles), and 10 nmol ATP.min^{-1}.mg^{-1} (ATP/O = 0.13 x mass$^{0.09}$, r^2 = 0.70, black circles). Values are means ± s.d. Dashed line illustrates the relationship between body mass and the ATP/O ratio calculated at 10 nmol ATP.min^{-1}.mg^{-1} in skeletal muscle mitochondria (data from Mélanie et al., 2019).

Figure 5. **Body mass dependence of mitochondrial enzyme activities and content.** A) Relationship between body mass and cytochrome-c oxidase activity measured in freshly isolated liver mitochondria (COX_{mito}). B) Relationships between body mass and citrate synthase activity measured in isolated mitochondria (CS_{mito}, black circles) or liver tissue (CS_{liver}, white circles). C) Relationship between body mass and mitochondrial content of liver (Q_{mito}, grey circles). Values are means ± s.d. from (n) independent preparations (see Materials and Methods for more details).

References

Barger, J.L., Brand, M.D., Barnes, B.M., Boyer, B.B. 2003. Tissue-specific depression of mitochondrial proton leak and substrate oxidation in hibernating arctic ground squirrels. Am. J. Physiol. 284, R1306-R1313.

Beavis, A.D., Lehninger, A.L. 1986. The upper and lower limits of the mechanistic stoichiometry of mitochondrial oxidative phosphorylation. Stoichiometry of oxidative phosphorylation. Eur. J. Biochem. 158, 315–322.

Boël, M., Romestaing, C., Duchamp, C., Veyrunes, F., Renaud, S., Roussel, D., Voituron, Y. 2020. Improved mitochondrial coupling as a response to high mass-specific metabolic rate in extremely small mammals. J. Exp. Biol. 223, jeb215558.

Bourguignon, A., Rameau, A., Toullec, G., Romestaing, C., Roussel, D. 2017. Increased mitochondrial energy efficiency in skeletal muscle after long-term fasting: its relevance to animal performance. J. Exp. Biol. 220, 2445–2451.

Brand, M.D. 2005. The efficiency and plasticity of mitochondrial energy transduction. Biochem. Soc. Trans. 33, 897–904.

Brand, M.D., Harper, M.E., Taylor, H.C. 1993. Control of the effective P/O ratio of oxidative phosphorylation in liver mitochondria and hepatocytes. Biochem. J. 291, 739-749.

Brand, M.D., Nicholls, D.G. 2011. Assessing mitochondrial dysfunction in cells. Biochem. J. 435, 297–312.

Brand, M.D., Turner, N., Ocloo, A., Else, P.L., Hulbert, A.J. 2003. Proton conductance and fatty acyl composition of liver mitochondria correlates with body mass in birds. Biochem. J. 376, 741–748.

Brown, J.C.L., Staples, J.F. 2010. Mitochondrial metabolism during fasting-induced daily torpor in mice. Biochim. Biophys. Acta 1797, 476-486.

Darveau, C.A., Suarez, R., Andrews, R., Hochachka, P. 2002. Allometric cascade as a unifying principle of body mass effects on metabolism. Nature 417, 166–170.

Dufour, S., Rousse, N., Canioni, P., Diolez, P. 1996. Top-down control analysis of temperature effect on oxidative phosphorylation. Biochem. J. 314, 743-751.

Else, P.L., Hulbert, A.J. 1985. Mammals: an allometric study of metabolism at tissue and mitochondrial level. Am. J. Physiol. 248, R415-R421.

Else, P.L., Brand, M.D., Turner, N., Hulbert, A.J. 2004. Respiration rate of hepatocytes varies with body mass in birds. J. Exp. Biol. 207, 2305–2311.

Emmet, B., Hochachka, P.W. 1981. Scaling of oxidative and glycolytic enzymes in mammals. Respir. Physiol. 45, 261-272.

Fontaine, E.M., Moussa, M., Devin, A., Garcia, J., Ghisolfi, J., Rigoulet, M., Leverve, X.M. 1996. Effect of polyunsaturated fatty acids deficiency on oxidative phosphorylation in rat liver mitochondria. Biochim.Biophys. Acta 1276, 181–187.

Fried, G.H., Tipton, S.R. 1953. Comparison of respiratory enzyme levels in tissues of mammals of different sizes. Proc. Soc. Exp. Biol. Med. 82, 531-532.

Fritz, S.A., Bininda-Emonds, O.R.P., Purvis, A. 2009. Geographical variation in predictors of mammalian extinction risk: big is bad, but only in the tropics. Ecol. Lett. 12, 538–549.

Glazier, D.S., 2008. Effects of metabolic level on the body size scaling of metabolic rate in birds and mammals. Proc. R. Soc. B 275, 1405–1410.

Hochachka, P.W., Darveau, C.A., Andrews, R.D., Suarez, R.K. 2003. Allometric cascade: a model for resolving body mass effects on metabolism. Comp. Biochem. Physiol. 134A, 675–691.

Hulbert, A.J., Else, P.L. 2000. Mechanisms underlying the cost of living in animals. Annu. Rev. Physiol. 62, 207–235.

Krebs, H.A. 1950. Body size and tissue respiration. Biochim. Biophys. Acta 4, 249-269.

Kunkel, H.O., Campbell, J.E. 1952. Tissue cytochrome oxidase activity and body weight. J. Biol. Chem. 198, 229-236.

Lang, G., Michal, G. 1974. D-glucose-6-phosphate and D-fructose-6-phosphate. In *Methods of enzymatic analysis* (ed. HU Bergmeyer), pp. 1238-1242.

Lombardi, A., Damon, M., Vincent, A., Goglia, F., Herpin, P. 2000. Characterisation of oxidative phosphorylation in skeletal muscle mitochondria subpopulations in pig: a study using top-down elasticity analysis. FEBS Lett. 475, 84-88.

Makarieva, A.M., Gorshkov, V.G., Li, B.L., Chown, S.L., Reich, P.B., Gavrilov, V.M. 2008. Mean mass-specific metabolic rates are strikingly similar across life's major domains: Evidence for life's metabolic optimum. Proc. Natl. Acad. Sci. USA 105, 16994–16999.

Medja, F., Allouche, S., Frachon, P., Jardel, C., Malgat, M., Mousson de Camaret, B., Slama, A., Lunardi, J., Mazat, J.P., Lombès, A. 2009. Development and implementation of standardized respiratory chain spectrophotometric assays for clinical diagnosis. Mitochondrion 9, 331-339.

Mélanie, B., Caroline, R., Yann, V., Damien, R. 2019. Allometry of mitochondrial efficiency is set by metabolic intensity. Proc. R. Soc. B 286, 20191693.

Mollica, M.P., Lionetti, L., Crescenzo, R., Tasso, R., Barletta, A., Liverini, G., Iossa, S. 2005. Cold exposure differently influences mitochondrial energy efficiency in rat liver and skeletal muscle. FEBS Lett. 579, 1978-1982.

Polymeropoulos, E.T., Heldmaier, G., Frappell, P.B., McAllan, B.M., Withers, K.W., Klingenspor, M., White, C.R., Jastroch, M. 2012. Phylogenetic differences of mammalian basal metabolic rate are not explained by mitochondrial basal proton leak. Proc. R. Soc. B 279, 185–193.

Porter, R.K. 2001. Allometry of mammalian cellular oxygen consumption. Cell. Mol. Life Sci. 58, 815–822.

Porter, R.K., Brand, M.D. 1993. Body mass dependence of H^+ leak in mitochondria and its relevance to metabolic rate. Nature 362, 628–630.

Porter, R.K., Brand, M.D. 1995. Causes of differences in respiration rate of hepatocytes from mammals of different body mass. Am. J. Physiol. 269, R1213-1224.

Porter, R.K., Hulbert, A.J., Brand, M.D. 1996. Allometry of mitochondrial proton leak: influence of membrane surface area and fatty acid composition. Am. J. Physiol. 271, R1550-R1560.

Rolfe, D.F.S., Hulbert, A.J., Brand, M.D. 1994. Characteristics of mitochondrial proton leak and control of oxidative phosphorylation in the major oxygen-consuming tissues of the rat. Biochim. Biophys. Acta 1118, 405-416.

Rolfe, D.F.S., Brand, M.D. 1996. Contribution of mitochondrial proton leak to skeletal muscle respiration and to standard metabolic rate. Am. J. Physiol. 271, C1380-1389.

Rolfe, D.F.S., Brown, G.C. 1997. Cellular energy utilization and molecular origin of standard metabolic rate in mammals. Physiol. Rev. 77, 731–758.

Rolfe, D.F.S., Newman, J.M., Buckingham, J.A., Clark, M.G., Brand, M.D. 1999. Contribution of mitochondrial proton leak to respiration rate in working skeletal muscle and liver and to SMR. Am. J. Physiol. 276, C692-699.

Roussel, D., Harding, M., Runswick, M.J., Walker, J.E., Brand, M.D. 2002. Does any yeast mitochondrial carrier have a native uncoupling protein function? J. Bioenerg. Biomembr. 34, 165-176.

Roussel, D., Dumas, J.F., Simard, G., Malthièry, Y., Ritz, P. 2004. Kinetics and control of oxidative phosphorylation in rat liver mitochondria after dexamethasone treatment. Biochem. J. 382, 491–499.

Roussel, D., Salin, K., Dumet, A., Romestaing, C., Rey, B., Voituron, Y. 2015. Oxidative phosphorylation efficiency, proton conductance and reactive oxygen species production of liver mitochondria correlates with body mass in frogs. J. Exp. Biol. 218, 3222–3228.

Salin, K., Teulier, L., Rey, B., Rouanet, J.L., Voituron, Y., Duchamp, C., Roussel, D. 2010. Tissue variation of mitochondrial oxidative phosphorylation efficiency in cold-acclimated ducklings. Acta Biochim. Pol. 57, 409–412.

Salin, K., Auer, S.K., Rey, B., Selman, C., Metcalfe, N.B. 2015. Variation in the link between oxygen consumption and ATP production, and its relevance for animal performance. Proc. R. Soc. B 282, 20151028.

Schmidt-Nielsen, K. 1984. In scaling: why is animal size so important? Cambridge, UK: Cambridge University Press.

Smith, R.E. 1956. Quantitative relations between liver mitochondria metabolism and total body weight in mammals. Ann. N.Y. Acad. Sci. 62, 405-421.

Teulier, L., Rouanet, J.L., Letexier, D., Romestaing, C., Belouze, M., Rey, B., Duchamp, C., Roussel, D. 2010. Cold-acclimation-induced non-shivering thermogenesis in birds is associated with upregulation of avian UCP but not with innate uncoupling or altered ATP efficiency. J. Exp. Biol. 213, 2476–2482.

Weibel, E.R., Bacigalupe, L.D., Schmitt, B., Hoppeler, H. 2004. Allometric scaling of maximal metabolic rate in mammals: muscle aerobic capacity as determinant factor. Respir. Physiol. Neurobiol. 140, 115–132.

White, C.R., Cassey, P., Blackburn, T.M. 2007. Allometric exponents do not support a universal metabolic allometry. Ecology 88, 315–323.

Declaration of interests

☒ The authors declare that they have no known competing financial interests or personal relationships that could have appeared to influence the work reported in this paper.

☐The authors declare the following financial interests/personal relationships which may be considered as potential competing interests:

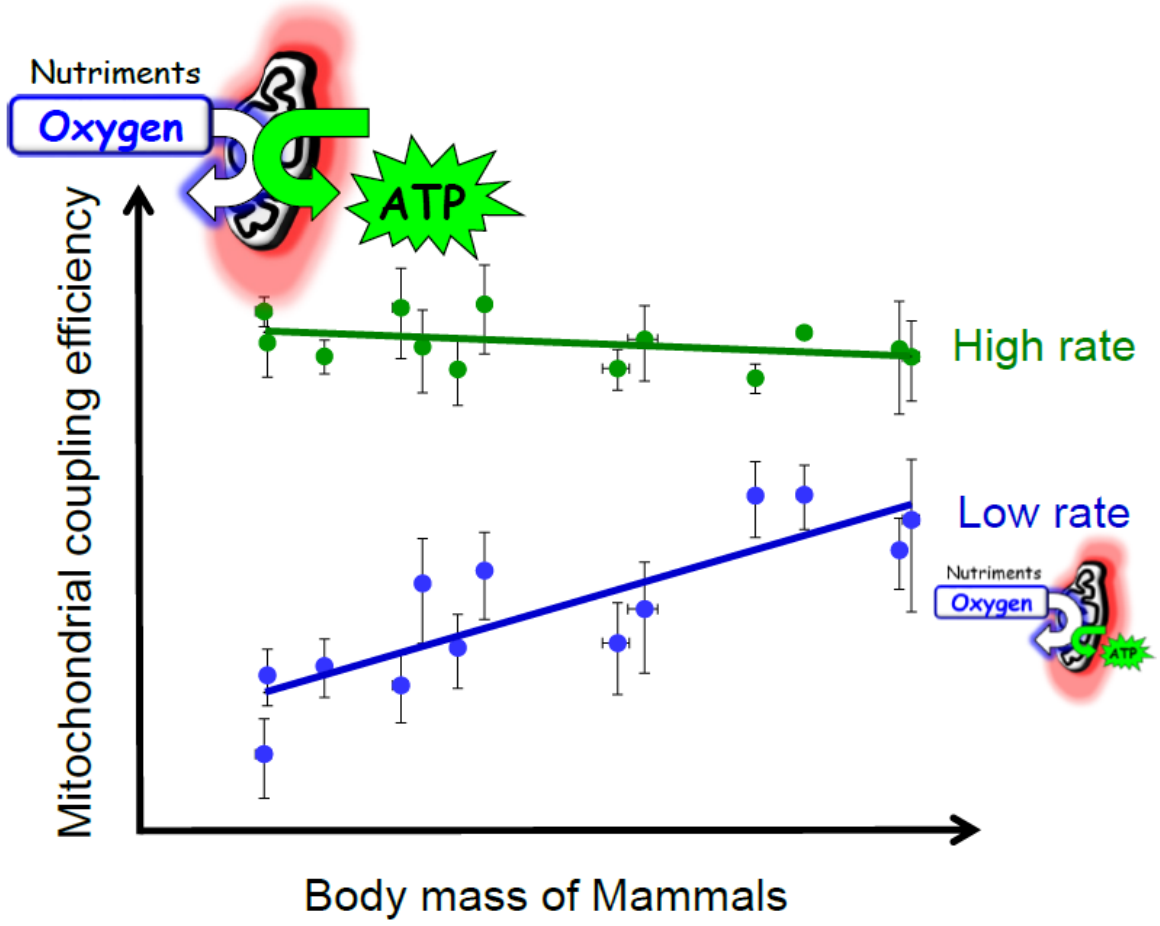
Nutriments
Oxygen
ATP
Mitochondrial coupling efficiency
High rate
Low rate
Nutriments
Oxygen
ATP
Body mass of Mammals

Highlights:

1. Mitochondrial oxygen consumption and ATP synthesis decrease when body mass rises
2. Citrate synthase and cytochrome-c oxidase activities decline when body mass rises
3. The liver mitochondria of smaller species are less efficient and more flexible
4. Metabolic intensity does not influence the allometry for mitochondrial efficiency